role of these cell surface proteins in pathogenesis. In addition, *Saccharomyces* may be a valuable tool for screening compounds that block fungal adhesion, a possible new avenue to antifungal therapy.

References and Notes

1. G. A. O'Toole, H. B. Kaplan, R. Kolter, *Annu. Rev. Microbiol.* **54**, 49 (2000).
2. J. W. Costerton, P. S. Stewart, E. P. Greenberg, *Science* **284**, 1318 (1999).
3. G. S. Baillie and L. J. Douglas, *Methods Enzymol.* **310**, 644 (1999).
4. For visualization of biofilms in wells of polystyrene plates, a protocol was adapted from G. A. O'Toole *et al.* [*Methods Enzymol.* **310**, 91 (1999)]; an equal volume of a solution of 1% (w/v) crystal violet was added to the cells and left for at least 15 min. The wells were washed repeatedly with H_20 and then photographed. Cells were also observed to adhere to polystyrene when not stained with crystal violet.
5. PVC 96 well plates (Falcon Microtest III flexible assay plates, 35-3912; Becton Dickinson) were used to test adhesion by essentially the same assay used for the polystyrene plates. Polypropylene microfuge tubes (Eppendorf flex-tube, 1.5 ml) were used to test adhesion to this type of plastic. In this instance, 400 μl of cells were used because the results were easier to judge macroscopically.
6. W. S. Lo, A. M. Dranginis, *Mol. Biol. Cell* **9**, 161 (1998).
7. B. Guo, C. A. Styles, Q. Feng, G. R. Fink, *Proc. Nat. Acad. Sci. U.S.A.* **97**, 12158 (2000).
8. H. Liu, C. A. Styles, G. R. Fink, *Genetics* **144**, 967 (1996).
9. An isogenic *MAT*α *flo11*Δ strain (TBR5) was generated in TBR1 (Σ1278b strain 10560-23C; *MAT*α, *ura3-52*, *his3::hisG*, *leu2::hisG*) by the protocol of M. S. Longtine *et al.* [*Yeast* **14**, 953 (1998)]. A polymerase chain reaction (PCR) fragment was used to replace the entire *FLO11* open reading frame with the kanamycin resistance gene. Other disruptants were generated in a similar manner (primers used for each disruptant can be found in *Science* Online at www.sciencemag.org/cgi/content/full/291/5505/878/DC1). The isogenic *MAT***a** strain (TBR2) was generated by transforming TBR1 with the pGAL::HO plasmid (B1377) and switching the mating type (*18*). The diploid *MAT***a**/α strain (TBR3) was generated by crossing TBR1 to TBR2. The *MAT***a** *flo11*Δ strain (TBR12) was generated by crossing TBR1 and TBR5 and sporulating the diploid and the *MAT***a**/α *flo11*Δ/*flo11*Δ strain (TBR13) was generated by crossing TBR5 and TBR12.
10. J. Recht, A. Martinez, S. Torello, R. Kolter, *J. Bacteriol.* **182**, 4348 (2000).
11. A. Martinez, S. Torello, R. Kolter, *J. Bacteriol.* **181**, 7331 (1999).
12. The results were obtained by growing 11 independent mats and measuring the diameter and number of spokes for each mat daily.
13. A *FLO11 MAT*α strain grown for 12 days at 25°C produced an average of 8.1×10^9 cells on YPD−0.3% agar and an average of 1.1×10^9 cells when grown on YPD−2% agar under the same conditions. A *MAT*α *flo11*Δ strain grown for 12 days at 25°C produced an average of 5.3×10^9 cells on YPD−0.3% agar and an average of 1.6×10^9 cells when grown on YPD−2% agar. Cell number was determined by transferring the cells from plates to 15-ml conical tubes (Falcon 35-2096) or microfuge tubes. The cell mass was suspended in water, the suspension was diluted, and the optical density at 600 nm (OD_{600}) was measured. The number represents the average of three plates for each strain at each agar concentration.
14. The mats formed on plates containing 0.25% glucose (low glucose) display mature spokes and hubs by day 4 and form a mat that is smaller in diameter than the mats formed on 2% glucose plates.
15. S. Rupp, E. Summers, H. J. Lo, H. Madhani, G. R. Fink, *EMBO J.* **18**, 1257 (1999).
16. R. L. Roberts, G. R. Fink, *Genes Dev.* **15**, 2974 (1994).
17. H. Liu, C. A. Styles, G. R. Fink, *Science* **10**, 1741 (1993).
18. T. Galitski, A. J. Saldanha, C. A. Styles, E. S. Lander, G. R. Fink, *Science* **285**, 251 (1999).
19. An aqueous-hydrocarbon biphasic hydrophobicity assay was adapted from a protocol by K. C. Hazen and B. W. Hazen [*J. Microbiol. Methods* **6**, 289 (1987)]. The cells were grown in liquid SC + 2% glucose to an OD_{600} of between 0.5 and 1.5, washed once in water, and resuspended in SC + 0.1% glucose to an OD_{600} of 0.5. After a stationary incubation of 3 hours at 25°C, the OD_{600} of the culture was measured. Then 1.2 ml of the culture was added to a 13 mm by 100 mm borosilicate glass tube. The cell suspension was overlaid with 600 μl of octane and the tube was vortexed for 3 min. The phases were allowed to separate and the OD_{600} was taken of the aqueous layer. The difference between the OD_{600} of the aqueous phase before and after addition of octane was used to determine the hydrophobicity.
20. M. Gagiano, D. van Dyk, F. F. Bauer, M. G. Labrechts, I. S. Pretorius, *Mol. Microbiol.* **31**, 103 (1999).
21. *FLO11* or *flo11*Δ cells were grown in SC + 2% glucose, harvested at an OD_{600} of 0.5 to 1.5, washed in water, and resuspended in SC + 0.1% glucose to an OD_{600} of 1.0. The cell suspension (30 μl) was then placed on a small rectangle (~5 mm by 5 mm) of ethanol-sterilized polystyrene (cut from petri dishes) and incubated in a petri dish at 30°C for 1.5 hours. The rectangle was then placed into a sterile well (Costar 3526, 24 well Cell Culture Cluster, Corning) containing 2 ml of SC + 0.1% glucose and grown for 18 to 24 hours at 30°C. The plastic rectangles were removed from the media, washed gently with water, and viewed under the microscope. The *FLO11* cell mass adhered to the rectangle in a dense multilayered film, whereas the *flo11*Δ cells did not.
22. *Candida albicans* formed a mat on 0.3% agar plates with a reproducible morphology that lacked spokes, but had a hub that was distinct from that found in *S. cerevisiae* mats. The mats formed by *C. glabrata* lacked hubs and spokes.
23. P. Sundstrom, *Curr. Opin. Microbiol.* **2**, 353 (1999).
24. B. P. Cormack, N. Ghori, S. Falkow, *Science* **285**, 578 (1999).
25. L. L. Hoyer, T. L. Payne, M. Bell, A. M. Myers, S. Scherer, *Curr. Genet.* **33**, 451 (1998).
26. Synthetic complete media and plates and YPD plates were made as described [C. Guthrie, G. R. Fink, *Methods Enzymol.* **194**, 12 (1991)] with the exception of the altered agar or glucose concentrations, which are specified in the text.
27. The adherence of cells was quantitated by solubilizing the crystal violet with 100 μl of 10% SDS. After 30 min, 100 μl of H_2O was added, the solution was mixed by pipetting, and 50 μl was transferred to a fresh polystyrene 96-well plate (Flat-bottom Nunc-MicroWell plate, 269620, Nalge Nunc International). The absorbance at 570 nm (A_{570}) was then monitored with a Dynatech MR600 microplate reader. In some experiments, after the cells were added, the plates were centrifuged at 3000 rpm for 5 min before the assay as a control for differences observed between strains due to differences in the rates at which the cells settled to the bottom of the plate. The general trends shown in Fig. 1, B and C, were observed regardless of whether or not the plates were centrifuged before the assay.

28. We thank D. Schneider, M. Lorenz, C. Styles, B. Guo, T. Galitski, and other members of the Fink lab for discussions and other valuable contributions and N. Watson for help with the scanning electron microscopy. Supported by NIH grants NIH 5 RO1 GM40266 (G.R.F.) and GM20565 (T.B.R.) and by the Corning Corporation.

17 October 2000; accepted 4 January 2001

Molecular Analysis of Commensal Host-Microbial Relationships in the Intestine

Lora V. Hooper,[1] Melissa H. Wong,[1] Anders Thelin,[2] Lennart Hansson,[2] Per G. Falk,[1,2] Jeffrey I. Gordon[1]*

Human beings contain complex societies of indigenous microbes, yet little is known about how resident bacteria shape our physiology. We colonized germ-free mice with *Bacteroides thetaiotaomicron*, a prominent component of the normal mouse and human intestinal microflora. Global intestinal transcriptional responses to colonization were observed with DNA microarrays, and the cellular origins of selected responses were established by laser-capture microdissection. The results reveal that this commensal bacterium modulates expression of genes involved in several important intestinal functions, including nutrient absorption, mucosal barrier fortification, xenobiotic metabolism, angiogenesis, and postnatal intestinal maturation. These findings provide perspectives about the essential nature of the interactions between resident microorganisms and their hosts.

Human beings harbor an incredibly complex and abundant ensemble of microbes. We are in contact with components of this microflora from birth, yet little is known about their influence on normal development and physiology. The human intestine is more densely populated with microorganisms than any other organ and is a site where the microflora may have a pronounced impact on our biology. We tested this idea at a molecular level using a simplified mouse model of the interactions between gut commensals and their host. In this model, adult germ-free animals are colonized with *Bacteroides thetaiotaomicron*. This anaerobe was chosen because it can be genetically manipulated and is a prominent member of the adult mouse and human

[1]Department of Molecular Biology and Pharmacology, Washington University School of Medicine, St. Louis, MO 63110, USA. [2]AstraZeneca R&D Mölndal, SE-431 83 Mölndal, Sweden.

*To whom correspondence should be addressed: E-mail: jgordon@molecool.wustl.edu

gut microflora. Moreover, *B. thetaiotaomicron* normally colonizes the distal small intestine (ileum) during the suckling-weaning transition, a time of rapid and pronounced functional maturation of the gut (*1*, *2*). We previously used this model to show how *B. thetaiotaomicron* regulates production of ileal epithelial fucosylated glycans for its own nutritional benefit (*3*).

As so little is known about the range of intestinal functions that are shaped by components of the microflora, we used high-density oligonucleotide arrays for analysis of the host transcriptional responses evoked by *B. thetaiotaomicron* colonization. In addition, we defined the cellular origins of a subset of these responses using laser-capture microdissection and real-time quantitative reverse transcriptase polymerase chain reaction (qRT-PCR) and examined the specificity of selected *B. thetaiotaomicron*–elicited responses using other members of the normal flora.

Adult male germ-free mice were inoculated with *B. thetaiotaomicron* and killed 10 days later (*4*). Ileal RNA was isolated from mice with $>10^7$ colony-forming units (CFU) of bacteria per milliliter of ileal contents. Earlier studies had shown that 10 days was sufficient to produce robust colonization of the ileum and that $\geq 10^7$ CFU/ml were necessary for full induction of fucosylated glycan expression in the ileal epithelium (*3*, *5*).

Table 1. Real-time qRT-PCR verification of selected colonization-associated changes in gene expression. Assays were performed with the pooled ileal RNA samples used for the microarray studies. Mean values for triplicate determinations ±1 SD are shown. See (*7*) for a comprehensive list of 71 genes that change with colonization.

Gene	Fold Δ (relative to germ-free)
Na^+/glucose cotransporter (SGLT-1)	2.6 ± 0.9
Colipase	6.6 ± 1.9
Liver fatty acid–binding protein (L-FABP)	4.4 ± 1.4
Metallothionein I (MT-I)	−5.4 ± 0.7
Polymeric immunoglobulin receptor (pIgR)	2.6 ± 0.7
Decay-accelerating factor (DAF)	5.7 ± 1.5
Small proline-rich protein 2a (sprr2a)	205 ± 64
Glutathione *S*-transferase (GST)	−2.1 ± 0.1
Multidrug resistance protein (Mdr1a)	−3.8 ± 1.0
Lactase-phlorizin hydrolase	−4.1 ± 0.6
Adenosine deaminase (ADA)	2.6 ± 0.5
Angiogenin-3	9.1 ± 1.8

Affymetrix Mu11K and Mu19K GeneChips, representing ~25,000 mouse genes, were used to compare ileal gene expression in age-matched germ-free and colonized animals.

mRNAs represented by 118 probe sets changed ≥twofold with colonization as defined by duplicate microarray hybridizations (*6*). Transcripts represented by 95 probe sets increased, whereas those represented by 23 probe sets decreased. Seventy-one genes, represented by 84 probe sets, were assigned to functional groups, whereas 34 transcripts were from uncharacterized genes or expressed sequence tag clusters (*7*). The microarray data reveal the unanticipated breadth of this commensal's impact on expression of genes involved in modulating fundamental intestinal functions.

Germ-free rodents require a higher caloric intake to maintain their weight than those with a microflora (*8*). Microarray analysis provided molecular insights into how *B. thetaiotaomicron* improves host nutrient absorption and processing. Colonization led to increased ileal levels of Na^+/glucose cotransporter (SGLT-1) mRNA (Table 1) (*7, 9*). Concerted increases were seen in several components of the host's lipid absorption machinery, including pancreatic lipase-related protein-2 (PLRP-2), colipase, a fatty acid–binding protein (L-FABP), and apolipoprotein A-IV (*7*) (Table 1). The prominent decrease in expression of fasting-induced adipose factor, a PPARα target that is repressed with fat feeding (*10*), provided further evidence for augmented lipid uptake in colonized mice. Micronutrient absorption also appears to be augmented by colonization, as evidenced by a threefold increase in expression of the high-affinity epithelial copper transporter (CRT1) and five- to sixfold decreases in expression of metallothioneins I and II and ferritin heavy chain, which sequester heavy metals within cells (*7*) (Table 1).

The DNA microarray and confirmatory qRT-PCR analyses measure host responses in a complex tissue composed of multiple cell types. An in vivo model will, unlike cell culture–based models, preserve the contributions of other cell lineages and environmental factors in shaping the response. The challenge is to recover the responding cell population, without perturbing its expressed mRNAs, so that its reaction to the microorganism can be characterized quantitatively. To define the cellular responses in our in vivo model, we combined laser-capture microdissection (LCM) with qRT-PCR. LCM was used to recover three cell populations from frozen sections of ileum (*11*), including epithelium from crypts (containing proliferating undifferentiated cells plus differentiated members of the Paneth cell lineage), epithelium overlying villi (containing postmitotic, differentiated members of the other three intestinal epithelial lineages), and mesenchyme underlying crypt-villus units [see (*7*) for LCM images]. Specific mRNAs in the LCM populations were quantified by RT-PCR.

Colipase is produced by pancreatic exocrine acinar cells, but we discovered that colipase is also expressed in ileal crypt epithelium, where it increased 10-fold upon *B. thetaiotaomicron* colonization (Fig. 1 and Table 1). Colipase plays a critical role in lipid metabolism by stimulating the activity of both pancreatic triglyceride lipase and pancreatic lipase-related protein-2 (*12*). Localization of colipase in the crypt epithelium and its regulation by a gut commensal reveal a previously unappreciated mechanism for lipid processing in the intestinal epithelium.

An intact mucosal barrier is critical for constraining resident intestinal microbes. Barrier disruption can provoke immune responses that cause pathology such as inflammatory bowel disease (*13*). *Bacteroides thetaiotaomicron* colonization produces no detectable inflammatory response, as judged by histologic surveys (*5*) and by the absence of a discernible induction or repression of immune response genes represented on the microarrays. An influx of immunoglobulin A (IgA)–producing B cells does occur in the ileal mucosa 10 days after introduction of *B. thetaiotaomicron* (*5*), but similar commensal-induced IgA responses have been shown to be T cell–independent and to enforce barrier integrity (*14*).

The influx of IgA-producing B cells was accompanied by increased expression of the polymeric immunoglobulin receptor (pIgR) that transports IgA across the epithelium (Table 1). There was augmented expression of the CRP-ductin gene encoding both a mucus layer component (MUCLIN) and a putative receptor for trefoil peptides (*15*, *16*). Decay-accelerating factor (DAF), an apical epithelial inhibitor of complement-mediated cytolysis, increased sixfold (*7*) (Table 1). Coincident enhancement of expression of these three genes should help prevent bacteria from crossing the epithelial barrier and avoid mucosal damage from activation of complement components in intestinal secretions.

The most pronounced response to *B. thetaiotaomicron* was an increase in small proline-rich protein-2 (sprr2a) mRNA (Table 1). sprr family members contribute to the barrier functions of squamous epithelia, both as a component of the cornified cell envelope and as cross-bridging proteins linked to desmosomal desmoplakin (*17*). LCM/qRT-PCR revealed that sprr2a mRNA is present in the epithelium, primarily on the villus rather than crypt, and that *B. thetaiotaomicron* elicits a 280-fold increase in its villus epithelial expression (Fig. 1). The epithelial sprr2a response suggests that this protein participates in forti-

fying the intestinal epithelial barrier in response to bacterial colonization.

Environmental and dietary constituents, as well as drugs, are detoxified in the intestine by oxidation or conjugation. Colonization produced a twofold decrease in expression of glutathione *S*-transferase, which conjugates glutathione to a variety of electrophiles, and a fourfold decrease in multidrug resistance protein–1a (Mdr1a), which exports glutathione-conjugated compounds from the epithelium (*18*) (Table 1). Debrisoquine hydroxylase (CYP2D2), which is involved in oxidative drug metabolism in humans (*19*), also declined threefold. These results indicate that colonization with *B. thetaiotaomicron* affects the host's capacity to metabolize xenobiotics and endogenous toxins.

Previous electrophysiological studies of germ-free and conventionally raised animals indicate that the microflora influences gut motility (*20*). Colonization led to two- to fivefold increases in mRNAs encoding L-glutamate transporter, L-glutamate decarboxylase (converts glutamate to γ-aminobutyric acid), vesicle-associated protein-33 (a synaptobrevin-binding protein involved in neurotransmitter release) (*21*), and enteric γ-actin and cysteine-rich protein-2 (muscle-specific proteins). These results suggest that *B. thetaiotaomicron* may affect components of the enteric nervous system (*22*) and motility.

Bacteroides thetaiotaomicron colonizes the mouse (and human) gut during the weaning period (*1*, *2*). This stage in postnatal gut development is marked by several maturational changes, including reductions in ileal epithelial lactase, which hydrolyzes milk sugar (*23*). Ileal epithelial lactase levels also fall as adult germ-free mice are colonized with *B. thetaiotaomicron* (Table 1). Adenosine deaminase (ADA) and polyamines are effectors of postnatal intestinal maturation (*24*, *25*). Colonization increased expression of both ADA and ornithine decarboxylase (ODC) antizyme, a regulator of polyamine synthesis (*26*), suggesting that commensals may perform an instructive role in postnatal intestinal maturation (*7*) (Table 1).

Colonization increased expression of angiogenin-3, a secreted protein with known angiogenic activity (*27*, *28*), and angiogenin-related protein, which does not have any apparent angiogenic activity (*29*). Angiogenin-3 was originally identified in NIH 3T3 fibroblasts (*27*), but little is known about its cellular origins in tissues. LCM/qRT-PCR revealed that angiogenin-3 mRNA is largely confined to the crypt epithelium and that colonization results in a sevenfold increase in its crypt expression (Fig. 1). This increase accounts for the change in expression defined by microarray and qRT-PCR analyses of total ileal RNA (Table 1). Localization of a secreted angiogenesis factor in the crypt epithelium puts it in a strategic position to function as an effector of several host responses to microbial colonization (e.g., enhanced absorption and distribution of nutrients).

Our findings raise two questions. Are similar host responses elicited by other components of the gut microflora, and do changes in the metabolic capacity of *B. thetaiotaomicron* affect ileal gene expression? To examine the first question, age-matched adult male mice (n = 4 to 8 mice per group) were colonized for 10 days with *B. thetaiotaomicron*, *Bifidobacterium infantis* (a prominent component of the preweaning human and mouse ileal flora and a commonly used probiotic), *Escherichia coli* K12 (a normal component of human intestinal flora), or a "complete" ileal/cecal microflora harvested from conventionally raised mice (*5*). qRT-PCR was used to compare mRNA levels in each group (all animals had $\geq 10^7$ CFU/ml ileal contents). Ileal expression of colipase and angiogenin-3 was induced after colonization with each of the three organisms and by the complete ileal/cecal flora (Fig. 2). Moreover, the ileal levels

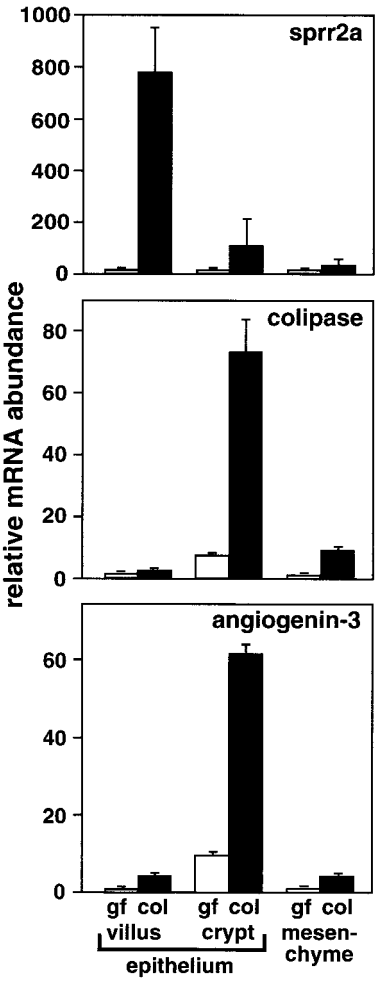

Fig. 1. Real-time qRT-PCR analysis of colonization-associated changes in gene expression in laser-capture microdissected ileal cell populations. Values are expressed relative to levels in germ-free mesenchyme (*9*). Each mRNA was assayed in triplicate in three to four independent experiments. Representative results (mean ± 1 SD) from pairs of germ-free (gf) and colonized (col) mice are plotted.

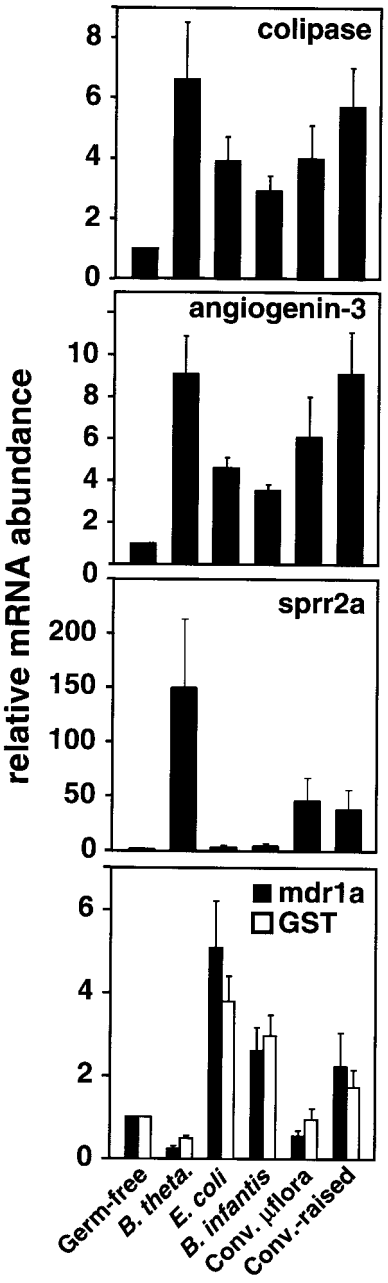

Fig. 2. Specificity of host responses to colonization with different members of the microflora. Germ-free mice were inoculated with one of the indicated organisms or with a complete ileal/cecal flora from conventionally raised mice (Conv. μflora) (*4*). Ileal RNAs, prepared from animals colonized at $\geq 10^7$ CFU/ml ileal contents 10 days after inoculation, were pooled, and levels of each mRNA shown were analyzed by real-time qRT-PCR. Mean values (±1 SD) for triplicate determinations are plotted.

of colipase and angiogenin-3 mRNAs in these ex–germ-free mice were comparable to those of age-matched mice conventionally raised since birth (Fig. 2). In contrast, the response of sprr2a to colonization depended on the colonizing species: *B. infantis* and *E. coli* produced only small increases (Fig. 2). Mdr1a and glutathione *S*-transferase also exhibited species-specific responses. *Bacteroides thetaiotaomicron* suppressed and *E. coli* and *B. infantis* stimulated expression of both genes, whereas the multicomponent ileal/cecal flora produced no significant (i.e., ≥twofold) change in levels of either mRNA compared with germ-free controls. The differing Mdr1a/GST responses suggest that variations in xenobiotic metabolism between individuals may arise, in part, from differences in their resident gut flora.

The only *B. thetaiotaomicron* genes currently known to link changes in bacterial metabolism with host responses are those involved in fucose utilization (*3*). Transposon-mediated mutagenesis of *fucI* (encoding fucose isomerase) blocks the organism's ability to use fucose as a carbon source and to signal fucosylated glycan production in the ileal epithelium (*3*). Microarray analysis of the host response to colonization revealed no appreciable differences between isogenic mutant and wild-type strains. This similarity extends to all genes in Table 1. Future identification of microbial factors that interlink microbial and host physiology will require characterization of changes in *B. thetaiotaomicron* gene expression as a function of colonization.

In summary, the studies described above provide a broad-based in vivo characterization of transcriptional responses to colonization with a prototypic gut commensal. Our results reveal that commensals are able to modulate expression of host genes that participate in diverse and fundamental physiological functions. The species selectivity of some of the colonization-associated changes in gene expression emphasizes how our physiology can be affected by changes in the composition of our indigenous microflora. The fusion of germ-free technology, functional genomics, and LCM/qRT-PCR makes it possible to use in vivo systems to quantify the impact of a microbial population on host cell gene expression.

References and Notes

1. W. E. C. Moore, L. V. Holdeman, *Appl. Microbiol.* **27**, 961 (1974).
2. T. Ushijima, M. Takahashi, K. Tatewaki, Y. Ozaki, *Microbiol. Immunol.* **27**, 985 (1983).
3. L. V. Hooper, J. Xu, P. G. Falk, T. Midtvedt, J. I. Gordon, *Proc. Natl. Acad. Sci. U.S.A.* **96**, 9833 (1999).
4. Age-matched groups of 7- to 15-week-old germ-free NMRI/KI mice were maintained in plastic gnotobiotic isolators on a 12-hour light cycle and given free access to an autoclaved chow diet (B&K Universal). Males were inoculated with *B. thetaiotaomicron* strain VPI-5482 (*3*), the isogenic Fu-4 strain lacking a functional *fucI* gene (*3*), *E. coli* K12, or *Bifidobacterium infantis* (ATCC15697). Mice were killed 10 days later, 2 hours after lights were turned on. The distal 1 cm of the small intestine was used to define CFU/ml ileal contents. The 3 cm of intestine just proximal to this segment was used to isolate total ileal RNA (Qiagen RNeasy kit).
5. L. Bry, P. G. Falk, T. Midtvedt, J. I. Gordon, *Science* **273**, 1380 (1996).
6. Total ileal RNA samples, prepared from four mice from three independent colonizations and from age-matched male germ-free controls ($n = 8$), were each pooled in equal amounts for generation of biotinylated cRNA targets. Two targets were prepared, independently, from 30 μg of each total cellular RNA pool (*30*). Each cRNA was hybridized to Mu11K and Mu19K chip sets according to Affymetrix protocols. The overall fluorescence intensity across each chip was scaled to a target intensity of 150. Pairwise comparisons of "germ-free" versus "colonized" expression levels were performed. A ≥twofold difference was considered significant if three criteria were met: The GeneChip software returned a difference call of Increased or Decreased, the mRNA was called Present by GeneChip software in either germ-free or colonized RNA, and the difference was observed in duplicate microarray hybridizations.
7. See supplemental material at http://gordonlab.wustl.edu.
8. B. S. Wostmann, C. Larkin, A. Moriarty, E. Bruckner-Kardoss, *Lab. Anim. Sci.* **33**, 46 (1983).
9. SYBR Green-based qRT-PCR (*31*) used gene-specific primers (*7*) and deoxyribonuclease-treated RNAs. Control experiments established that amplicons were derived from cDNA and not from primer-dimers or genomic DNA. Signals were normalized to glyceraldehyde 3-phosphate dehydrogenase mRNA. Normalized data were used to quantitate relative levels of a given mRNA in germ-free and colonized ileums ($\Delta\Delta C_T$ analysis; User Bulletin #2, ABI Prism 7700 Sequence Detection System).
10. S. Kersten *et al.*, *J. Biol. Chem.* **275**, 28488 (2000).
11. Seven-micrometer-thick sections were cut from ileums harvested immediately after the death of three sets of germ-free and colonized mice that were independent of those used for microarray profiling. LCM was conducted with the PixCell II system (Arcturus, 7.5-μm-diameter laser spot) and RNA was prepared (Stratagene RNA Micro-Isolation Kit; protocols in http://dir.nichd.nih.gov/lcm/protocol.htm).
12. M. E. Lowe, M. H. Kaplan, L. Jackson-Grusby, D. D'Agostino, M. J. Grusby, *J. Biol. Chem.* **273**, 31215 (1998).
13. P. G. Falk, L. V. Hooper, T. Midtvedt, J. I. Gordon, *Microbiol. Mol. Biol. Rev.* **62**, 1157 (1998).
14. A. J. Macpherson *et al.*, *Science* **288**, 2222 (2000).
15. R. C. DeLisle, M. Petitt, K. S. Isom, D. Ziemer, *Am. J. Physiol.* **275**, G219 (1998).
16. L. Thim, E. Mørtz, *Regul. Pept.* **90**, 61 (2000).
17. P. M. Steinert, L. N. Marekov, *Mol. Biol. Cell* **10**, 4247 (1999).
18. R. W. Johnstone, A. A. Ruefli, M. J. Smyth, *Trends Biochem. Sci.* **25**, 1 (2000).
19. M. Ingelman-Sundberg, M. Oscarson, R. A. McLellan, *Trends Pharmacol. Sci.* **20**, 342 (1999).
20. E. Husebye, P. M. Hellstrom, T. Midtvedt, *Dig. Dis. Sci.* **39**, 946 (1994).
21. P. A. Skehel, R. Fabian-Fine, E. R. Kandel, *Proc. Natl. Acad. Sci. U.S.A.* **97**, 1101 (2000).
22. M. T. Liu, J. D. Rothstein, M. D. Gershon, A. L. Kirchgessner, *J. Neurosci.* **17**, 4764 (1997).
23. S. D. Krasinski *et al.*, *Am. J. Physiol.* **267**, G584 (1994).
24. G. D. Lux, L. J. Marton, S. B. Baylin, *Science* **210**, 195 (1980).
25. J. M. Chinsky *et al.*, *Differentiation* **42**, 172 (1990).
26. J. Nilsson, S. Koskiniemi, K. Persson, B. Grahn, I. Holm, *Eur. J. Biochem.* **250**, 223 (1997).
27. X. Fu, M. P. Kamps, *Mol. Cell Biol.* **17**, 1503 (1997).
28. X. Fu, W. G. Roberts, V. Nobile, R. Shapiro, M. P. Kamps, *Growth Factors* **17**, 125 (1999).
29. V. Nobile, B. L. Vallee, R. Shapiro, *Proc. Natl. Acad. Sci. U.S.A.* **93**, 4331 (1996).
30. C. K. Lee, R. G. Klopp, R. Weindruch, T. A. Prolla, *Science* **285**, 1390 (1999).
31. N. Steuerwald, J. Cohen, R. J. Herrera, C. A. Brenner, *Mol. Hum. Reprod.* **5**, 1034 (1999).

32. We thank C. Hong, E. Skogman, and B. Basta for technical assistance. This work was funded by NIH grant DK30292 and AstraZeneca.

16 October 2000; accepted 4 January 2001

Protein Design of an HIV-1 Entry Inhibitor

Michael J. Root, Michael S. Kay, Peter S. Kim*†

Human immunodeficiency virus type–1 (HIV-1) membrane fusion is promoted by the formation of a trimer-of-hairpins structure that brings the amino- and carboxyl-terminal regions of the gp41 envelope glycoprotein ectodomain into close proximity. Peptides derived from the carboxyl-terminal region (called C-peptides) potently inhibit HIV-1 entry by binding to the gp41 amino-terminal region. To test the converse of this inhibitory strategy, we designed a small protein, denoted 5-Helix, that binds the C-peptide region of gp41. The 5-Helix protein displays potent (nanomolar) inhibitory activity against diverse HIV-1 variants and may serve as the basis for a new class of antiviral agents. The inhibitory activity of 5-Helix also suggests a strategy for generating an HIV-1 neutralizing antibody response that targets the carboxyl-terminal region of the gp41 ectodomain.

Infection by HIV-1, the virus that causes AIDS, requires fusion of the viral and cellular membranes (*1–3*). This membrane-fusion process is mediated by the viral envelope glycoprotein complex (gp120/gp41) and receptors on the target cell. Binding of gp120/gp41 to cell-surface receptors (CD4 and a coreceptor, such as CCR5 or CXCR4) triggers a series of conformational changes in the gp120/gp41 oligomer that ultimately lead to formation of a trimer-of-hairpins structure in gp41 (Fig. 1A).

The trimer-of-hairpins is a common structural element involved in the fusion process of many enveloped viruses, suggesting a critical role for this motif in promoting mem-